1-1-2008

Measurement of Deeply Virtual Compton Scattering Beam-Spin Asymmetries

F. X. Gilrod

Angela Biselli
Fairfield University, abiselli@fairfield.edu

CLAS Collaboration

Peer Reviewed

Published Citation

F. X. Girod et al. [CLAS Collaboration], "Measurement of Deeply Virtual Compton Scattering Beam-Spin Asymmetries," Physical Review Letters 100.16 (2008) DOI: 10.1103/PhysRevLett.100.162002

Measurement of Deeply Virtual Compton Scattering Beam-Spin Asymmetries

F. X. Girod,[1,2] R. A. Niyazov,[2,32] H. Avakian,[2] J. Ball,[1] I. Bedlinskiy,[3] V. D. Burkert,[2] R. De Masi,[1,4] L. Elouadrhiri,[2] M. Garçon,[1,*] M. Guidal,[4] H. S. Jo,[4] K. Joo,[12] V. Kubarovsky,[2,32] S. V. Kuleshov,[3] M. MacCormick,[4] S. Niccolai,[4] O. Pogorelko,[3] F. Sabatié,[1] S. Stepanyan,[2] P. Stoler,[32] M. Ungaro,[12] B. Zhao,[12] M. J. Amaryan,[31] P. Ambrozewicz,[15] M. Anghinolfi,[21] G. Asryan,[40] H. Bagdasaryan,[31] N. Baillie,[29] J. P. Ball,[6] N. A. Baltzell,[35] V. Batourine,[23] M. Battaglieri,[21] M. Bellis,[9] N. Benmouna,[17] B. L. Berman,[17] A. S. Biselli,[9,14] L. Blaszczyk,[16] S. Bouchigny,[4] S. Boiarinov,[2] R. Bradford,[9] D. Branford,[13] W. J. Briscoe,[17] W. K. Brooks,[2] S. Bültmann,[31] C. Butuceanu,[39] J. R. Calarco,[28] S. L. Careccia,[31] D. S. Carman,[2] L. Casey,[10] S. Chen,[16] L. Cheng,[10] P. L. Cole,[19] P. Collins,[6] P. Coltharp,[16] D. Crabb,[38] V. Crede,[16] N. Dashyan,[40] E. De Sanctis,[20] R. De Vita,[21] P. V. Degtyarenko,[2] A. Deur,[2] K. V. Dharmawardane,[31] R. Dickson,[9] C. Djalali,[35] G. E. Dodge,[31] J. Donnelly,[18] D. Doughty,[11,12] M. Dugger,[6] O. P. Dzyubak,[35] H. Egiyan,[2] K. S. Egiyan,[40] L. El Fassi,[5] P. Eugenio,[16] G. Fedotov,[27] G. Feldman,[17] H. Funsten,[39] G. Gavalian,[31] G. P. Gilfoyle,[34] K. L. Giovanetti,[22] J. T. Goetz,[7] A. Gonenc,[15] R. W. Gothe,[35] K. A. Griffioen,[39] N. Guler,[31] L. Guo,[2] V. Gyurjyan,[2] K. Hafidi,[5] H. Hakobyan,[40] C. Hanretty,[16] F. W. Hersman,[28] K. Hicks,[30] I. Hleiqawi,[30] M. Holtrop,[28] C. E. Hyde,[24,31] Y. Ilieva,[17] D. G. Ireland,[18] B. S. Ishkhanov,[27] E. L. Isupov,[27] M. M. Ito,[2] D. Jenkins,[37] J. R. Johnstone,[18] H. G. Juengst,[17,31] N. Kalantarians,[31] J. D. Kellie,[18] M. Khandaker,[29] W. Kim,[23] A. Klein,[31] F. J. Klein,[10] A. V. Klimenko,[31] M. Kossov,[3] Z. Krahn,[9] L. H. Kramer,[15,2] J. Kuhn,[9] S. E. Kuhn,[31] J. Lachniet,[9,31] J. M. Laget,[2] J. Langheinrich,[35] D. Lawrence,[26] T. Lee,[28] K. Livingston,[18] H. Y. Lu,[35] N. Markov,[12] P. Mattione,[33] M. Mazouz,[25] B. McKinnon,[18] B. A. Mecking,[2] M. D. Mestayer,[2] C. A. Meyer,[9] T. Mibe,[30] B. Michel,[24] K. Mikhailov,[3] M. Mirazita,[20] R. Miskimen,[26] V. Mokeev,[27,2] K. Moriya,[9] S. A. Morrow,[1,4] M. Moteabbed,[15] E. Munevar,[17] G. S. Mutchler,[33] P. Nadel-Turonski,[17] R. Nasseripour,[15,35] G. Niculescu,[22] I. Niculescu,[22] B. B. Niczyporuk,[2] M. R. Niroula,[31] M. Nozar,[2] M. Osipenko,[21,27] A. I. Ostrovidov,[16] K. Park,[35] E. Pasyuk,[6] C. Paterson,[18] S. Anefalos Pereira,[20] J. Pierce,[38] N. Pivnyuk,[3] D. Pocanic,[38] S. Pozdniakov,[3] J. W. Price,[8] S. Procureur,[1] Y. Prok,[38,2] D. Protopopescu,[18] B. A. Raue,[15,2] G. Ricco,[21] M. Ripani,[21] B. G. Ritchie,[6] G. Rosner,[18] P. Rossi,[20] J. Salamanca,[19] C. Salgado,[20] J. P. Santoro,[10] V. Sapunenko,[2] R. A. Schumacher,[9] V. S. Serov,[3] Y. G. Sharabian,[2] D. Sharov,[27] N. V. Shvedunov,[27] E. S. Smith,[2] L. C. Smith,[38] D. I. Sober,[10] D. Sokhan,[13] A. Stavinsky,[3] S. S. Stepanyan,[23] B. E. Stokes,[16] I. I. Strakovsky,[17] S. Strauch,[17,35] M. Taiuti,[21] D. J. Tedeschi,[35] A. Tkabladze,[30,17] S. Tkachenko,[31] C. Tur,[35] M. F. Vineyard,[36] A. V. Vlassov,[3] E. Voutier,[25] D. P. Watts,[18] L. B. Weinstein,[31] D. P. Weygand,[2] M. Williams,[9] E. Wolin,[2] M. H. Wood,[35] A. Yegneswaran,[2] L. Zana,[28] J. Zhang,[31] and Z. W. Zhao[35]

(CLAS Collaboration)

[1]*CEA-Saclay, Service de Physique Nucléaire, 91191 Gif-sur-Yvette, France*
[2]*Thomas Jefferson National Accelerator Facility, Newport News, Virginia 23606, USA*
[3]*Institute of Theoretical and Experimental Physics, Moscow, 117259, Russia*
[4]*IPNO, Université Paris-Sud, CNRS/IN2P3, 91406 Orsay, France*
[5]*Argonne National Laboratory, Argonne, Illinois 60439, USA*
[6]*Arizona State University, Tempe, Arizona 85287-1504, USA*
[7]*University of California at Los Angeles, Los Angeles, California 90095-1547, USA*
[8]*California State University, Dominguez Hills, Carson, California 90747, USA*
[9]*Carnegie Mellon University, Pittsburgh, Pennsylvania 15213, USA*
[10]*Catholic University of America, Washington, D.C. 20064, USA*
[11]*Christopher Newport University, Newport News, Virginia 23606, USA*
[12]*University of Connecticut, Storrs, Connecticut 06269, USA*
[13]*Edinburgh University, Edinburgh EH9 3JZ, United Kingdom*
[14]*Fairfield University, Fairfield Connecticut 06824, USA*
[15]*Florida International University, Miami, Florida 33199, USA*
[16]*Florida State University, Tallahassee, Florida 32306, USA*
[17]*The George Washington University, Washington, D.C. 20052, USA*
[18]*University of Glasgow, Glasgow G12 8QQ, United Kingdom*
[19]*Idaho State University, Pocatello, Idaho 83209, USA*
[20]*INFN, Laboratori Nazionali di Frascati, 00044 Frascati, Italy*
[21]*INFN, Sezione di Genova, 16146 Genova, Italy*
[22]*James Madison University, Harrisonburg, Virginia 22807, USA*
[23]*Kyungpook National University, Daegu 702-701, South Korea*

[24]LPC Clermont-Ferrand, Université Blaise Pascal, CNRS-IN2P3, 63177 Aubière, France
[25]LPSC, Université Joseph Fourier, CNRS/IN2P3, INPG, 38026 Grenoble, France
[26]University of Massachusetts, Amherst, Massachusetts 01003, USA
[27]Moscow State University, General Nuclear Physics Institute, 119899 Moscow, Russia
[28]University of New Hampshire, Durham, New Hampshire 03824-3568, USA
[29]Norfolk State University, Norfolk, Virginia 23504, USA
[30]Ohio University, Athens, Ohio 45701, USA
[31]Old Dominion University, Norfolk, Virginia 23529, USA
[32]Rensselaer Polytechnic Institute, Troy, New York 12180-3590, USA
[33]Rice University, Houston, Texas 77005-1892, USA
[34]University of Richmond, Richmond, Virginia 23173, USA
[35]University of South Carolina, Columbia, South Carolina 29208, USA
[36]Union College, Schenectady, New York 12308, USA
[37]Virginia Polytechnic Institute and State University, Blacksburg, Virginia 24061-0435, USA
[38]University of Virginia, Charlottesville, Virginia 22901, USA
[39]College of William and Mary, Williamsburg, Virginia 23187-8795, USA
[40]Yerevan Physics Institute, 375036 Yerevan, Armenia
(Received 6 December 2007; published 23 April 2008)

The beam-spin asymmetries in the hard exclusive electroproduction of photons on the proton ($\vec{e}p \to ep\gamma$) were measured over a wide kinematic range and with high statistical accuracy. These asymmetries result from the interference of the Bethe-Heitler process and of deeply virtual Compton scattering. Over the whole kinematic range (x_B from 0.11 to 0.58, Q^2 from 1 to 4.8 GeV^2, $-t$ from 0.09 to 1.8 GeV^2), the azimuthal dependence of the asymmetries is compatible with expectations from leading-twist dominance, $A \simeq a\sin\phi/(1 + c\cos\phi)$. This extensive set of data can thus be used to constrain significantly the generalized parton distributions of the nucleon in the valence quark sector.

DOI: 10.1103/PhysRevLett.100.162002 PACS numbers: 13.60.Fz, 13.40.Gp, 13.60.Hb, 14.20.Dh

The structure of the nucleon, the lightest of all baryonic states, has been studied in the past using two complementary approaches. Elastic electron scattering measures form factors which reflect the spatial shape of charge distributions [1], while deep inelastic scattering provides access to parton distribution functions that encode, in a fast moving nucleon, the momentum fraction carried by the constituents [2]. The formalism of generalized parton distributions (GPDs) [3–5] unifies these approaches and provides much greater insight into nucleon structure [6,7], through the coherence between states of different longitudinal momentum fractions, the correlation between transverse coordinates and longitudinal momentum of the partons [8], the distribution of forces exerted upon partons [9] (information inconceivable to obtain just a few years ago) and the angular momentum carried by each type of parton [4].

Deeply virtual Compton scattering (DVCS) on the proton ($\gamma^* p \to \gamma p$), in the Bjorken regime where the photon scattering occurs at the quark level, is the process of choice to attain an experimental determination of GPDs. Pioneering observations of DVCS [10–16], though of limited experimental accuracy, are all compatible with a description of the observables in terms of GPDs, both in the gluon and in the quark sectors. Moreover, a recent precise experiment [17] gave good indications of the onset of scaling in this process at relatively modest values of the γ^* virtuality.

In this context, this work presents the first systematic and precise exploration of a sensitive observable, the beam-spin asymmetry of the reaction $\vec{e}p \to ep\gamma$. Neglecting a twist-3 DVCS term, this asymmetry arises from the interference between the Bethe-Heitler (BH) and DVCS processes (that is, where the photon is emitted by the electron or by the target nucleon, respectively). At leading twist, it is primarily sensitive to the imaginary part of the DVCS amplitude and thus to a specific linear combination of the proton GPDs H, $\tilde{H}$ and E, with arguments $x(= \pm\xi)$, ξ and t. Each proton GPD involves a weighted sum over the quark flavors. The beam-spin asymmetry is defined as

$$A = \frac{d^4\overrightarrow{\sigma} - d^4\overleftarrow{\sigma}}{d^4\overrightarrow{\sigma} + d^4\overleftarrow{\sigma}}, \tag{1}$$

where the arrows correspond to beam helicity $+1$ and -1. It depends on Q^2, x_B, t, defined in Fig. 1, and on the angle ϕ between the leptonic and hadronic planes. Harmonic decompositions of the cross sections $d^4\sigma$, divided among contributions from BH, DVCS, and interference (INT) terms, have been proposed [18,19]. In the notation of Ref. [19], the cross sections, up to some kinematic factors, can be expressed in terms of the ϕ-harmonics $c_n^S\cos n\phi$ and $s_n^S\sin n\phi$, with n from 0 to 3 and $S =$ BH, INT, or DVCS. At the twist-2 level, which according to Ref. [17] is largely dominant at least up to $|t| = 0.35$ GeV^2, the numerator of Eq. (1) gets a contribution from s_1^{INT} only, while the denominator contains the coefficients c_0^{INT}, c_1^{INT} and c_0^{DVCS}, in addition to $c_n^{\mathrm{BH}}(n = 0, 1, 2)$ calculable in QED in terms of the proton elastic form factors. At leading twist,

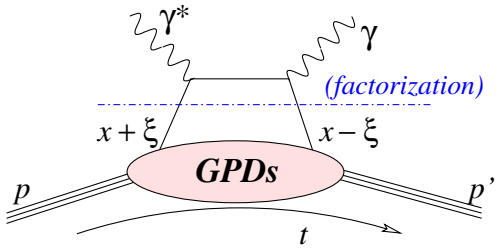

FIG. 1 (color online). Schematic representation of the leading-order handbag diagram contribution to DVCS, where x is the average longitudinal momentum fraction of the active quark in the initial and final states [measured in terms of the average hadron momentum $(p + p')/2$], while 2ξ is their difference; it is related to the Bjorken scaling variable by $\xi \simeq x_B/(2 - x_B)$. The squared four-momentum transfer to the target is $t = (p' - p)^2$, and the squared four-momentum of the virtual photon is $-Q^2$.

one obtains

$$A = \frac{a \sin\phi}{1 + c\cos\phi + d\cos 2\phi}, \tag{2}$$

where the parameters a, c and d may be expressed in terms of the above mentioned harmonic coefficients. The DVCS and INT harmonic coefficients may in turn be written in terms of Compton form factors related to the corresponding GPD by

$$\mathrm{Re}\,\mathcal{H} = \mathrm{P}\int_{-1}^{1} dx \left[\frac{2x}{\xi^2 - x^2}\right] H(x, \xi, t), \tag{3}$$

$$\frac{1}{\pi}\mathrm{Im}\mathcal{H} = H(\xi, \xi, t) - H(-\xi, \xi, t), \tag{4}$$

up to corrections of order of the strong coupling constant, with similar expressions for $\tilde{\mathcal{H}}$, $\mathcal{E}$ and $\tilde{\mathcal{E}}$. The GPD H yields the dominant contribution to the harmonic coefficients considered above. Neglecting the small contributions from the three other GPDs, one can express the beam-spin asymmetry A in terms of only $\mathrm{Re}\mathcal{H}$ and $\mathrm{Im}\mathcal{H}$. Thus in this approximation, which is expected to hold for small values of $|t|$, the parameters a, c and d of Eq. (2) are uniquely related to the imaginary and real parts of the Compton form factor $\mathcal{H}$, yielding, respectively, the GPD H at points $x = \pm\xi$ and the principal value integral of Eq. (3). Going beyond this approximation requires additional theoretical or experimental constraints on the other GPDs.

The experiment took place in Hall B of Jefferson Laboratory, using the CEBAF 5.77 GeV electron beam (with average polarization $P = 0.794$), a 2.5 cm-long liquid-hydrogen target and the CLAS spectrometer [20]. The three final-state particles from the reaction $ep \to ep\gamma$ were detected. For this purpose, a new inner calorimeter (IC) was added to the standard CLAS configuration, 55 cm downstream from the target, in order to detect 1 to 5 GeV photons emitted between 4.5° and 15° with respect to the beam direction. This calorimeter was built of 424 tapered lead-tungstate crystals, 16 cm-long and with an average cross-sectional area of 2.1 cm^2, read out with avalanche photodiodes and associated low-noise preamplifiers. The whole IC was operating at a stabilized temperature of 17 °C, and monitored with laser light homogeneously distributed on all crystals. The calorimeter was calibrated several times during the run using the two-photon decay of neutral pions. Energy and angle resolutions of 4.5% and 4 mrad (for 1 GeV photons) were achieved. In conjunction, a specifically designed superconducting solenoid was used to trap around the beam axis the background originating from Møller electrons, while permitting detection of the recoil protons up to 60°.

Events were selected if an electron had generated the trigger, one and only one proton was identified and only one photon (above an energy threshold of 150 MeV) was detected in either the IC or the standard CLAS calorimeter EC. Electrons were identified through signals in the EC and in the Čerenkov counters. From time-of-flight information, track length and momentum, protons were unambiguously distinguished from positive pions over the whole momentum range of interest. All clusters detected in the IC were assumed to originate from photons, while additional time-of-flight information was used in the EC to separate photons from neutrons. For all three final-state particles, fiducial cuts were applied to exclude detector edges.

Operating at a luminosity of $2 \times 10^{34}\ \mathrm{cm}^{-2}\,\mathrm{s}^{-1}$ (a record for CLAS), the accidental coincidences were negligibly small, as well as the pile-up probability in the IC, except for the most forward photons below 6°. Events considered here include the kinematic requirements: $Q^2 > 1\ \mathrm{GeV}^2$, $\gamma^* p$ invariant mass $W > 2$ GeV and scattered electron energy $E' > 0.8$ GeV. The mere selection of the three final-state particles results in the observation of characteristic peaks in distributions of all kinematic variables expressing the conservation of total four-momentum in the reaction $ep \to ep\gamma$, as exemplified by the dotted curves in Fig. 2. Requiring in addition a missing transverse momentum smaller than 0.09 GeV, an angle between the $\gamma^* p'$ and $\gamma p'$ planes smaller than 1.5°, a photon detected within 1.2° of the direction inferred from the detected electron and proton, and a maximal missing energy E_X of 0.3 GeV, results in clean peaks for the events of interest. These kinematic cuts are to some extent redundant (except for the background to be discussed below) and are quoted here for the case where the emitted photon is detected in the IC, that is for 92% of the events. In the case of photons detected in the EC, these cuts are about twice as large because of the poorer resolution.

In spite of this selection, a contamination of events originating from the $ep \to ep\pi^0$ reaction, followed by the subsequent asymmetric decay of the neutral pion, is always possible. For these events, one of the photons is not detected, because it is either below threshold or outside the calorimeters' acceptance. This physical background is es-

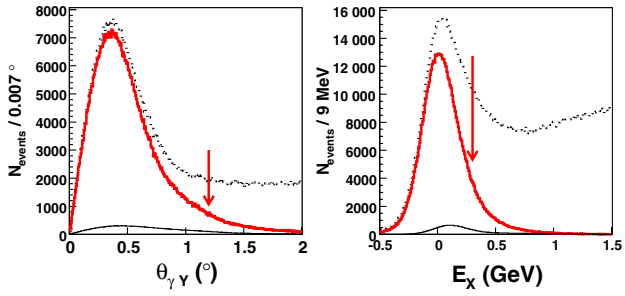

FIG. 2 (color online). Distributions in cone angle $\theta_{\gamma Y}$ for the $ep \to epY$ reaction (left) and in missing energy E_X for the $ep \to ep\gamma X$ reaction (right), before (black dotted curve) and after (red solid) all kinematic cuts discussed in the text but the one on the histogrammed variable, given by the location of the arrow. The thin solid black line represents the physical background, calculated from measured $ep \to ep\pi^0$ events. The distributions are integrated over all kinematic variables and apply to the case where the photon is detected in the IC.

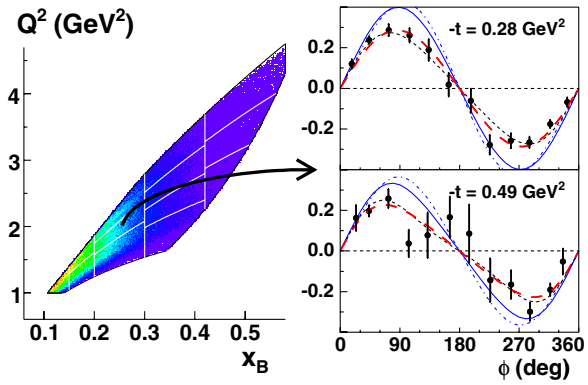

FIG. 3 (color online). Left: kinematic coverage and binning in the (x_B, Q^2) space. Right: $A(\phi)$ for 2 of the 62 (x_B, Q^2, t) bins, corresponding to $\langle x_B \rangle = 0.249$, $\langle Q^2 \rangle = 1.95$ GeV^2, and two values of $\langle t \rangle$. The red long-dashed curves correspond to fits with Eq. (2) (with $d = 0$). The black dashed curves correspond to a Regge calculation [27]. The blue curves correspond to the GPD calculation described in the text, at twist-2 (solid) and twist-3 (dot-dashed) levels, with H contribution only.

timated using the number $N^{2\gamma}_{\pi^0}$ of measured $ep \to ep\pi^0$ events, identified unambiguously when the two photons are detected [21], and multiplying it by the ratio of acceptances $(\mathrm{Acc})^{1\gamma}_{\pi^0}/(\mathrm{Acc})^{2\gamma}_{\pi^0}$, where the "$1\gamma$" acceptance is to be understood with the photon satisfying all the $ep \to ep\gamma$ event selection cuts. This ratio, which depends mostly on the photon geometrical cuts and on the relevant resolutions, has been calculated with the standard CLAS simulation package and a simplified fast Monte Carlo method, the two results being used to evaluate the corresponding systematic uncertainties. The background proportion f varies between 1 and 25% depending on the kinematic bin, 5% in average. The number of $ep \to ep\gamma$ events is then, for each beam-helicity state and for each elementary bin in the four kinematic variables (see below), $\vec{N} = \vec{N}_{\mathrm{ep}\to\mathrm{ep}\gamma X} - [(\mathrm{Acc})^{1\gamma}_{\pi^0}/(\mathrm{Acc})^{2\gamma}_{\pi^0}]\vec{N}^{2\gamma}_{\pi^0}$, and the asymmetry $A = (\vec{N} - \overleftarrow{N})/P(\vec{N} + \overleftarrow{N})$. Finally, radiative corrections were applied [22]. These tend to increase the asymmetries very slightly.

The data were divided into 13 bins in the (x_B, Q^2) space as per Fig. 3, five bins in $-t$ (defined by the bin limits 0.09, 0.2, 0.4, 0.6, 1 and 1.8 GeV^2) and 12 30° bins in ϕ. Bin-size corrections were applied. Whether integrated in t or in each t-bin (Fig. 3), the ϕ-distributions were always found to be compatible with Eq. (2) with $d = 0$. The parameter d is expected to be smaller than 0.05 over our kinematic range, and indeed was found compatible with zero, within statistical accuracy, when including it in the fit. The deviation from a pure sine function as $|t|$ increases is seen in all (x_B, Q^2) bins and results in the parameter c becoming negative [23]. The parameter a is the best estimate of $A(90°)$ and is represented in Fig. 4. Point-to-point systematic uncertainties arise mostly from the background subtraction: $\Delta A_b = (A - A_{\pi^0})\Delta f/(1 - f)$, where the relative error on f is conservatively estimated to be 30% and A_{π^0} is the asymmetry for the reaction $ep \to ep\pi^0$, ranging between 0.04 and 0.11 at 90° [21]. The sensitivity of the results to the event selection cuts was studied as well. From these two sources of information, the systematic uncertainty on a was inferred to be 0.010, independent of x_B, Q^2, and t. An overall normalization uncertainty arises from the

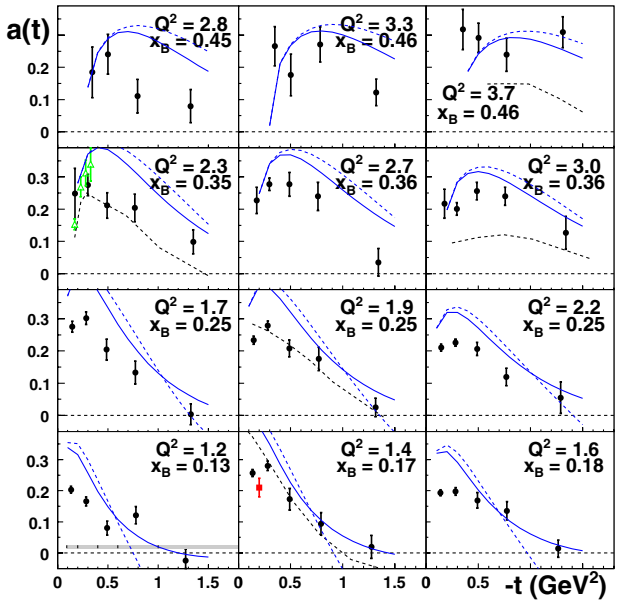

FIG. 4 (color online). $a = A(90°)$ as a function of $-t$. Each individual plot corresponds to a bin in (x_B, Q^2). Systematic uncertainties and bin limits are illustrated by the gray band in the lower left plot. Black circles are from this work. Previous results are from Ref. [12] (red square) or extracted from cross section measurements [17] (green triangles), at similar—but not equal—values of $\langle x_B \rangle$ and $\langle Q^2 \rangle$. See Fig. 3 caption for curve legend.

uncertainty in the beam polarization (3.5%). Additional details on the experiment and on the data analysis may be found in Ref. [23].

The wide kinematic coverage of the present data is important for global analyses of $ep \to ep\gamma$ observables and for a model-independent extraction of DVCS amplitudes. The beam-spin asymmetries are especially, but not uniquely, sensitive to the GPD H. When combined with other observables more sensitive to $\tilde{H}$ and E, as well as with unpolarized cross sections, it will be possible to obtain the real and imaginary parts of the Compton form factors of all GPDs, as defined in Eqs. (3) and (4). Additional theoretical work is also required, to clarify how power-suppressed contributions not included in Ref. [19] would affect the relations between observables and GPDs [24]. Presently, GPDs may be calculated using theoretical models based on constituent quarks, on a chiral quark-soliton description of the nucleon, on light-cone or other frameworks. The first moments of GPDs are being calculated using lattice QCD techniques. But none of these calculations are developed to the point of making the link to DVCS observables. Alternatively, constrained parameterizations have been used to make predictions of DVCS beam-spin asymmetries. Following Refs. [25,26], such a parameterization of the GPD H may be

$$H = \sum_q e_q^2 \left\{ \int_{-1}^{+1} d\beta \int_{-1+|\beta|}^{1-|\beta|} d\alpha\, \delta(x-\beta-\xi\alpha)\, \mathfrak{h}^q(\beta,\alpha,t) + \theta\left(1-\frac{x^2}{\xi^2}\right) D^q\left(\frac{x}{\xi},t\right)\right\}, \quad (5)$$

with

$$\mathfrak{h}^q(\beta,\alpha,t) = q(\beta)\pi_b(\beta,\alpha)e^{-\alpha_1'(1-\beta)t}, \quad (6)$$

where e_q and $q(\beta)$ are the electric charge and unpolarized parton distribution for quark flavor q, π_b a profile function [25] and α_1' is a Regge slope adjusted to recover the proton form factor F_1 from the first moment of the GPD. Equation (6) extends the ansatz of Ref. [26] for the t dependance to nonzero values of ξ. The D term in Eq. (5) is calculated within a quark-soliton chiral model [7]. Using predetermined parameters, the calculations of beam-spin asymmetries yield the solid and dot-dashed curves in Figs. 3 and 4, without and with a twist-3 term calculated in the Wandzura-Wilczek approximation [7]. The predictions overestimate the asymmetries at low $|t|$, especially for small values of x_B and/or Q^2. Variations of the parameter b entering the profile function π_b do not resolve this problem, which may indicate that double distributions are not flexible enough to reproduce this behavior.

Alternatively, description of the process in terms of meson (or more generally Regge trajectory) exchanges has been attempted [27,28]. DVCS may be viewed as ρ production followed by $\rho - \gamma$ coupling in vacuum or in the nucleon field. In addition to pole contributions in the t channel [29], the box diagram that takes into account ρ-nucleon intermediate states has been evaluated [27]. This calculation, represented by the dashed curves in Figs. 3 and 4, is in fair agreement with our results up to $Q^2 = 2.3$ GeV^2. The significance of this dual description (Regge vs handbag) remains to be fully investigated.

In summary, the most extensive set of DVCS data to date has been obtained with the CLAS spectrometer, augmented with specially designed small-angle photon calorimeter and solenoid. Beam-spin asymmetries were extracted in the valence quark region, as a function of all variables describing the reaction. Present parameterizations of GPDs describe reasonably well, but not perfectly, the main features of the data. The measured kinematic dependences will put stringent constraints on any DVCS model, and, in particular, on the generalized parton distributions in the nucleon.

We would like to thank B. Hervieu (DAPNIA-Saclay), Ph. Rosier (IPN-Orsay) and their collaborators for the skillful engineering of the new equipment. We acknowledge the outstanding efforts of the staff of the Accelerator and Physics Divisions at Jefferson Lab that made this experiment possible. We also acknowledge useful discussions with D. Müller. This work was supported in part by the French Centre National de la Recherche Scientifique and Commissariat à l'Energie Atomique, the U. S. Department of Energy and National Science Foundation, the Italian Istituto Nazionale di Fisica Nucleare, the Korean Science and Engineering Foundation, the U.K. Engineering and Physical Science Research Council. The Jefferson Science Associates (JSA) operates the Thomas Jefferson National Accelerator Facility for the United States Department of Energy under Contract No. DE-AC05-06OR23177.

*michel.garcon@cea.fr

[1] R. Hofstadter (1961), URL http://nobelprize.org/nobel_prizes/physics/laureates/1961/hofstadter-lecture.html.
[2] J. I. Friedman, H. W. Kendall, and R. E. Taylor, Rev. Mod. Phys. **63**, 573 (1991).
[3] D. Müller, D. Robaschik, B. Geyer, F. M. Dittes, and J. Hořejši, Fortschr. Phys. **42**, 101 (1994).
[4] X.-D. Ji, Phys. Rev. Lett. **78**, 610 (1997).
[5] A. V. Radyushkin, Phys. Rev. D **56**, 5524 (1997).
[6] J. P. Ralston and B. Pire, Phys. Rev. D **66**, 111501 (2002).
[7] K. Goeke, M. V. Polyakov, and M. Vanderhaeghen, Prog. Part. Nucl. Phys. **47**, 401 (2001).
[8] M. Burkardt, Phys. Rev. D **62**, 071503(R) (2000); **66**, 119903(E) (2002).
[9] M. V. Polyakov, Phys. Lett. B **555**, 57 (2003).
[10] C. Adloff *et al.* (H1 Collaboration), Phys. Lett. B **517**, 47 (2001).
[11] A. Airapetian *et al.* (HERMES Collaboration), Phys. Rev. Lett. **87**, 182001 (2001).

[12] S. Stepanyan *et al.* (CLAS Collaboration), Phys. Rev. Lett. **87**, 182002 (2001).
[13] S. Chekanov *et al.* (ZEUS Collaboration), Phys. Lett. B **573**, 46 (2003).
[14] A. Aktas *et al.* (H1 Collaboration), Eur. Phys. J. C **44**, 1 (2005).
[15] S. Chen *et al.* (CLAS Collaboration), Phys. Rev. Lett. **97**, 072002 (2006).
[16] A. Airapetian *et al.* (HERMES Collaboration), Phys. Rev. D **75**, 011103(R) (2007).
[17] C. Mũnoz Camacho *et al.* (Jefferson Lab Hall A Collaboration), Phys. Rev. Lett. **97**, 262002 (2006).
[18] M. Diehl, T. Gousset, B. Pire, and J. P. Ralston, Phys. Lett. B **411**, 193 (1997).
[19] A. V. Belitsky, D. Müller, and A. Kirchner, Nucl. Phys. **B629**, 323 (2002).
[20] B. A. Mecking *et al.* (CLAS Collaboration), Nucl. Instrum. Methods Phys. Res., Sect. A **503**, 513 (2003).
[21] R. De Masi *et al.* (CLAS Collaboration), Phys. Rev. C **77**, 042201(R) (2008).
[22] M. Vanderhaeghen *et al.*, Phys. Rev. C **62**, 025501 (2000); code adapted to DVCS with GPD model by P. Guichon (2007).
[23] F. X. Girod, Ph.D. thesis, Université Louis Pasteur, Strasbourg, France [Institution Report No. DAPNIA-06-18-T 2006].
[24] D. Müller (private communication) and work in progress.
[25] A. V. Radyushkin, in *At the Frontier of Particle Physics-Handbook of QCD*, edited by M. Shifman (World Scientific, Singapore, 2001), p. 1037.
[26] M. Guidal, M. V. Polyakov, A. V. Radyushkin, and M. Vanderhaeghen, Phys. Rev. D **72**, 054013 (2005).
[27] J. M. Laget, Phys. Rev. C **76**, 052201 (2007).
[28] A. Szczepaniak, J. Londergan, and F. Llanes-Estrada, arXiv:0707.1239.
[29] F. Cano and J. M. Laget, Phys. Lett. B **551**, 317 (2003); **571**, 260(E) (2003).